DOI:
10.1002/ajmg.a.38342

Document Version
Peer reviewed version

American Journal of Medical Genetics Part A

Autopsy findings in EPG5-related Vici syndrome with antenatal onset

Journal:	*American Journal of Medical Genetics: Part A*
Manuscript ID	16-1142.R1
Wiley - Manuscript type:	Clinical Report
Date Submitted by the Author:	n/a
Keywords:	Vici syndrome, EPG5 gene, Fetal medicine, Neuropathology
Search Terms:	

Complete List of Authors:
Touraine, Renaud; CHU-Hôpital Nord , Service de Génétique
Laquerrière, Annie; rouen university hospital, pathology
Petcu, Carmen Adina ; CHU de Saint-Etienne, Service d'anatomie et cytologie pathologiques
Marguet, Florent; rouen university hospital, pathology
Byrne, Susan; Guy' & St Thomas' NHS Foundation Trust Evelina Children's Hospital, Department of Paediatric Neurology
Mein, Rachael; Guy's and Saint Thomas' NHS Foundation Trust, Diagnostic DNA Laboratory
Yau, Michael; Guy's and Saint Thomas' NHS Foundation Trust, Diagnostic DNA Laboratory
Mohammed, Shehla; Guy's and St Thomas's NHS Foundation Trust, Deaprtment of Clinical Genetics
Guibaud, Laurent; Hospices Civils de Lyon, Département d'Imagerie Pédiatrique et Fœtale
Gautel, Mathias; King's College London, Randall Division for Cell and Molecular Biophysics
Jungbluth, Heinz; Guy' & St Thomas' NHS Foundation Trust Evelina Children's Hospital, Department of Paediatric Neurology; King's College, London, UK, Clinical Neuroscience Division

Autopsy findings in *EPG5*-related Vici syndrome with antenatal onset

[1]Renaud Touraine, [2]Annie Laquerrrière, [3]Carmen-Adina Petcu, [2]Florent Marguet, [4]Susan Byrne, [5]Rachael Mein, [5]Shu Yau, [6]Shehla Mohammed, [7]Laurent Guibaud, [8]Mathias Gautel,[4,8-9]Heinz Jungbluth

[1]CHU-Hôpital Nord, Service de Génétique, Saint Etienne, France; [2]Pathology Laboratory, Rouen University Hospital, Rouen, France and Normandie Univ, UNIROUEN, NéoVasc, Rouen, 76000, France ; [3]CHU-Hôpital Nord, Service d'Anatomopathologie, Saint Etienne, France ; [4]Department of Paediatric Neurology, Neuromuscular Service, Evelina's Children Hospital, Guy's & St. Thomas' Hospital NHS Foundation Trust, London, UK; [5]GSTS Pathology, Guy's Hospital, London, UK; [6]Department of Clinical Genetics, Guy's Hospital, London, UK; [7]Imagerie pédiatrique et fœtale, Hôpital Femme Mère Enfant, Lyon-Bron, France ; [8]Randall Division for Cell and Molecular Biophysics, Muscle Signaling Section, King's College, London; [9]Department of Basic and Clinical Neuroscience, IoPPN, King's College London, London, UK

Running title: Fetal Vici syndrome

Address for correspondence:

Professor Heinz Jungbluth
Children's Neurosciences Centre,
F01 – Staircase D South Wing,
St Thomas' Hospital,
Westminster Bridge Road,
London SE1 7EH, UK
Phone: 00442071883998
e-mail: Heinz.Jungbluth@gstt.nhs.uk

ABSTRACT

Vici syndrome is one of the most extensive inherited human multisystem disorders and due to recessive mutations in *EPG5* encoding a key autophagy regulator with a crucial role in autophagosome-lysosome fusion. The condition presents usually early in life, with features of severe global developmental delay, profound failure to thrive, (acquired) microcephaly, callosal agenesis, cataracts, cardiomyopathy, hypopigmentation and combined immunodeficiency. Clinical course is variable but usually progressive and associated with high mortality.

Here we present a fetus, offspring of consanguineous parents, in whom callosal agenesis and other developmental brain abnormalities were detected on fetal US and subsequent MRI scan in the second trimester. Post mortem examination performed after medically indicated termination of pregnancy confirmed CNS abnormalities and provided additional evidence for skin hypopigmentation, nascent cataracts and hypertrophic cardiomyopathy. Genetic testing prompted by a suggestive combination of features revealed a homozygous *EPG5* mutation (c.5870-1G>A) predicted to cause aberrant splicing of the *EPG5* transcript.

Our findings expand the phenotypical spectrum of *EPG5*-related Vici syndrome and suggest that this severe condition may already present *in utero*. Whilst callosal agenesis is not an uncommon finding in fetal medicine, additional presence of hypopigmentation, cataracts and cardiomyopathy is rare and should prompt *EPG5* testing.

KEY WORDS:

Vici syndrome; Fetal medicine; Neuropathology; *EPG5* gene

INTRODUCTION

Vici syndrome [MIM#242840], originally described by Dr Carlo Dionisi-Vici in 1988 [Vici et al., 1988], is one of the most severe multisystem disorders in humans and characterized by profound global developmental delay, failure to thrive, (acquired) microcephaly, callosal agenesis, cataracts, cardiomyopathy, hypopigmentation and combined immunodeficiency. More than 50 genetically resolved patients have been reported [Byrne et al., 2016] since the discovery of *EPG5* as the causative gene [Cullup et al., 2013]. *EPG5* encodes ectopic P-granules autophagy protein 5 (EPG5), an ubiquitously expressed protein critically implicated in autophagy [Cullup et al., 2013], a tightly regulated and highly conserved lysosomal degradative pathway with important roles in cellular homeostasis including infection defence, quality control of proteins and organelles, and metabolic adaptation. *EPG5*-related Vici syndrome (subsequently referred to as Vici syndrome) shows marked genetic homogeneity, and the likelihood of identifying causative *EPG5* mutations is in excess of 95% if all of the 8 clinical features listed above are present [Byrne et al., 2016]. The vast majority of *EPG5* mutations are truncating loss-of-function mutations. Severity appears to be determined by the residual amount of functional *EPG5* protein, as demonstrated for the recurrent *EPG5* p.Gln336Arg mutation associated with a milder clinical phenotype and variable effects on splicing, resulting in both normal and abnormal isoforms [Kane et al., 2016].

Clinical presentation in Vici syndrome typically starts from the neonatal period or infancy, followed by a variably progressive course [Byrne et al. 2016]. Although many of the diagnostic features are already seen at presentation, failure to thrive, microcephaly, cataracts, cardiomyopathy and combined immunodeficiency often only evolve over time. Here we report detailed post mortem findings from a fetus with Vici syndrome. Evolution of callosal agenesis, microcephaly, eye anomalies and cardiomyopathy already *in utero* suggest a much wider phenotypical spectrum associated with EPG5 deficiency than previously recognized.

CLINICAL REPORT

Clinical history: During the pregnancy of a 35-year-old woman of North African origin (Gravida 2, Para 1) antenatal ultrasound scan (US) at 22 weeks gestation revealed isolated agenesis of the corpus callosum (ACC). Initial pregnancy stages had been uneventful and the initial 1st trimester antenatal US examination had been normal. Further US examinations at 26 and 28 weeks plus 4 days gestation revealed additional abnormalities comprising delayed brain maturation with a small cerebellum (transverse cerebellar diameter 26.8 mm at 26 weeks gestation - 10th centile - and 28.9 mm at 28 weeks plus 4 days gestation - < 10th centile). Occipito-frontal circumference at the same time points was normal (at 236 and 256mm, respectively). Thorax was narrow but heart was structurally normal. Fetal brain MRI performed at 29 weeks gestation confirmed ACC and demonstrated lack of gyration development with abnormal Sylvian fissures and enlarged pericerebral spaces, as well as pontocerebellar hypoplasia involving mainly the brainstem (Fig. 1A and B). Due to the potential severity of the prognosis, parents opted for a medically indicated termination of pregnancy, performed at 30.5 weeks gestation after approval by the local Prenatal Diagnosis Centre and in accordance with French law. In the family history, the fetus was the second offspring of consanguineous, first cousin Moroccan parents. Their first child, a girl, had died at 9 months of age from acute necrotizing encephalopathy of unknown aetiology. The maternal grandmother had cataracts from the age of 50. Two of her siblings (which were also siblings of the paternal grandmother) had isolated vitiligo. The father of these siblings (the maternal great-grandfather of the index case) had visual impairment secondary to cataracts from 50 years of age. There was no familial history of previous fetal loss or anomalies, neurodegenerative disorders, or neoplasias.

Post mortem examination: Post mortem examination was performed with informed written consent from both parents according to standardized protocols (summarized in Supplemental

file S1), including X-rays, clinical photographs, and macroscopic and microscopic examination of all viscera. *General post mortem examination* revealed an eutrophic male fetus with a weight of 1570g (50th percentile). The crown–rump length was 26cm and the crown–heel length was 41.5cm. Head circumference was 28cm (5th percentile). Skeletal measurements were in accordance with gestational age, and no skeletal abnormalities were detected. A pale skin complexion and mild dysmorphic facial features were noted, including down slanting palpebral fissures, a small mouth with thin lips, prominent philtrum, high arched palate, retrognathism and large ears. External male genitalia appeared small. Spleen, liver and thymus weights were between the 50th and 75th percentile for gestational age. *Examination of the heart* revealed dilatation of the right ventricle with an enlarged tricuspid valve (0.7 cm). Weight of the heart was 18.7g (>95th percentile), suggestive of hypertrophy. Brain weight was 179g (<3rd percentile) suggestive of microcephaly. Macroscopic *examination of the brain* (Fig. 1) confirmed delayed gyration with abnormally wide, triangular-shaped Sylvian fissures, corresponding to a developmental stage of 25 weeks gestation (Fig.1C). The superior temporal gyrus was not normally formed and had a dimple-shaped appearance, as typically observed before 27 weeks' gestation, and asymmetric pachygyria predominant in the temporal and occipital areas. All these data supported the overall impression of microcephaly with a simplified gyral pattern. On coronal supratentorial sections, all brain structures were macroscopically normal, except for the corpus callosum which appeared absent (Fig. 1D). At the infratentorial level, delayed foliation of the vermis with absent tertiary folia was noted. The corpus callosum was composed of very few fibres, with very thin Probst Bundles (Fig. 2A and B), and premature regression of the ganglionic eminences. Histologically, no other lesions were observed in any structures of the cerebral hemispheres and of the infratentorial nuclei, the basal ganglia, internal capsule, hippocampi, as well as olivary and brainstem nuclei. Cortical lamination was normal for gestation.

Cortical microcolumnar dysplasia, sometimes present in primitive autosomal-recessive microcephaly with simplified gyral pattern, was not observed. There was no accumulation of PAS positive material in cortical neurons. Despite vermis simplified foliation (Fig. 2C), the cerebellar cortex had a normal lamination. Pyramidal tracts were strongly hypoplastic and fragmented in the mesencephalon (Fig. 2D) and the pons, and virtually absent in the medulla (Fig.2E), with delayed myelination and almost absent myelin in the brainstem (Fig. 2F). *Eye examination* revealed increased anterior lens epithelium thickness on the left, corresponding to a nascent anterior subcapsular cataract, instead of the monolayered anterior lens cuboidal epithelium typically seen at a comparable gestation (Fig. 2G, insert). Of note, pigmentation of the retina and ciliary processes was normal (Fig. 2H). At the macroscopic level, other organ anomalies were not found, except for an accessory spleen, a very common finding.

Histological examination of heart and psoas muscle did not reveal any abnormalities. Neither rimmed nor autophagic vacuoles were visualized using spectrin or LC3, and no accumulation of p62 and ubiquitin could be identified in the sarcoplasm. Ultrastructural examination did not reveal any vacuoles, abnormal mitochondria or glycogen excess. Thymic lymphocytic depletion, a not unusual finding on fetal autopsy, was noted.

Genetic studies: Prenatal testing for chromosomal rearrangements using Array-CGH (60k Agilent) had been normal. Culture of amniotic cells, cryopreserved fetal tissue and peripheral parental blood samples were obtained with the informed consent of both parents. Genomic DNA was extracted using standardized procedures. Testing for *EPG5* mutations by DNA sequencing revealed an apparently homozygous variant (c.5870-1G>A), predicted to cause aberrant splicing of the *EPG5* transcript. Both parents as well as their previously deceased child were heterozygous for the mutation.

DISCUSSION

To our knowledge this the first case of Vici syndrome with antenatal onset and documentation of agenesis of the corpus callosum (ACC) and other characteristic features on fetal US, MRI and post mortem analyses. ACC has an estimated prevalence of 1.4 per 10,000 [Glass et al., 2008] and may be isolated or associated with other brain developmental anomalies [Santo et al., 2012]. The structure of the corpus callosum should be formed by 20 weeks, however it continues to thicken after that [Tang et al., 2009]. Corpus callosal anomalies can thus in principle be detected after 20 weeks gestational age, but accuracy depends on the imaging modality applied [Glenn et al., 2005]: ACC may often be missed in low risk fetal US imaging studies especially if there are no other associated brain developmental abnormalities [Tang et al., 2009], however, those may be identified in almost two third of cases who have subsequent fetal MRI scans [Glenn et al., 2005]. Brain MRI abnormalities in living Vici syndrome patients comprise consistent findings of ACC, pontine hypoplasia likely due to hypoplastic and disorganized pyramidal tracts, delayed myelination, reduced white matter bulk and underopercularisation of the Sylvian fissures probably related to insufficient interneuron production as reflected by premature regression of the ganglionic eminences; Other variably present features include thalamic signal changes, simplified sulcation and cerebellar abnormalities [Byrne et al., 2016; Cullup et al., 2013]; our findings suggest that at least some of these features may already present antenatally. In addition to ACC and delayed gyration already detected on fetal imaging, other cardinal Vici syndrome features, in particular nascent cataracts and a cardiomyopathy, were detected on autopsy in our case. Whilst ACC as such is not an uncommon finding in fetal medicine, the combination of above features is rarely found and should thus prompt *EPG5* testing. MIDAS syndrome (MIM#309801), Yunis-Varon syndrome (MIM#216340) or 1p36 chromosome deletion syndrome (MIM#607872) are other conditions that may present antenatally with similar

overlapping features but that can be distinguished either through confirmation of the underlying chromosomal abnormality on CGH array, or the presence of additional features unusual in the context of Vici syndrome, such as microphtalmia (plus linear skin defects) in MIDAS, and cleido-cranial dysplasia with digital anomalies in Yunis-Varon syndrome.

To our knowledge, autopsies have only been reported in 4 unrelated infants with *EPG5*-related Vici syndrome to date [Byrne et al., 2016; Miyata et al., 2014; Rogers et al., 2011; Vici et al., 1988]. The key findings from these reports (summarized in Supplemental Table ST1) suggest that microcephaly, ACC, pontocerebellar abnormalities and pyramidal tract hypoplasia are consistently present. Although the combination of ACC, microcephaly and pontocerebellar hypoplasia is not specific as such and may indeed occur in other pontocerebellar hypoplasia syndromes (for example, the form secondary to *AMPD2* loss [Marsh et al., 2015]), neurohistological findings in Vici syndrome radically differ from those found in other forms. Of note, the marked hypoplasia of the pyramidal tracts in the mesencephalon (Fig. 2D) and the pons, and their virtual absence in the medulla (Fig.2E) corresponds to findings in one case where post mortem was performed postnatally, and observations in epg5-deficient mice, where marked neuronal loss is observed in pyramidal layer V of the motor and sensory cortices [Zhao et al., 2013]. Ocular abnormalities, in particular cataracts, are one of the defining features of Vici syndrome and undoubtedly represent a key autopsy finding both on antenatal and postnatal post mortem [Rogers et al., 2011] examination. Skin hypopigmentation is more difficult to evaluate in a deceased fetus or infant, but was present in our case and may be a valuable supportive feature. In Vici syndrome patients, cardiac presentations may comprise structural heart anomalies present from birth (including atrial or ventricular septal defects, mitral valve malformations and aortic coarctation), and/or signs of a hypertrophic and/or dilated cardiomyopathy [Byrne et al., 2016]. Our case had signs of an antenatal-onset cardiomyopathy but, in contrast to cases

where post mortem was performed postnatally [Miyata et al., 2014; Rogers et al., 2011], did not show hypertrophy of cardiomyocytes and excessive vacuolation, suggesting that those features may reflect the accumulative effects of failing autophagy over time rather than being universally present already at the early stages of development. Dysregulated autophagy has been well-documented in muscle and fibroblasts from Vici syndrome patients [Cullup et al., 2013], but as a dynamic adaptive process may require time and the strains of postnatal life to exert a detectable downstream effect on skeletal and cardiac muscles on the histopathological level. Along similar lines, absence of abnormal histopathological skeletal muscle features, a common finding in infants and children with Vici syndrome, may reflect the early stage of muscle development in our case compared to the age when biopsies were performed in the patients previously reported. The choice of muscle investigated is another potential explanation for the observed lack of histopathologigal muscle abnormalities, considering that the iliopsoas muscles is commonly spared in other neuromuscular conditions and was also found to be normal on a previous post mortem examination of an infant with Vici syndrome [Miyata et al., 2014]).

The homozygous *EPG5* mutation (c.5870-1G>A) identified in our patient is predicted to cause aberrant splicing in keeping with a common mechanism in other Vici syndrome cases. Interestingly and corresponding to observations in other families, we did note subtle clinical signs, in particular an apparent increase in early-onset cataracts and/or vitiligo, in (putative) carriers of the familial *EPG5* mutation. This observation is not easily reconciled with the autosomal-recessive inheritance pattern of Vici syndrome, but may reflect a rather complex effect on splicing as recently demonstrated for the recurrent *EPG5* p.Gln336Arg mutation, resulting in a number of different splice isoforms with gain-of-function, loss-of-function and normal function all possible consequences [Kane et al., 2016].

In conclusion, our case expands the spectrum of Vici syndrome, suggesting onset of 3 characteristic features – callosal agenesis, cataracts and cardiomyopathy - already *in utero* from midgestation. In contrast to their consistent presence on biopsies performed in living infants or on postnatal post mortem, histopathological features indicative of defective autophagy were not observed on fetal skeletal and cardiac muscle samples, suggesting that those may only evolve postnatally as a reflection of failing autophagic adaptation. The presence of subtle manifestations, in particular early-onset cataracts and vitiligo, in (putative) carriers of the familial *EPG5* mutation is noteworthy. We recommend that the antenatal discovery of ACC should prompt a careful search for other radiological features of Vici syndrome such as (ponto)cerebellar hypoplasia and delayed gyration on fetal brain MRI, and abnormalities of the eyes and heart, in particular cataracts, cardiac malformations and signs of an (evolving) cardiomyopathy. *EPG5* analysis should be part of the genetic assessment of the fetus presenting with ACC, in particular if other sugestive features are present.

References

Byrne S, Jansen L, JM UK-I, Siddiqui A, Lidov HG, Bodi I, Smith L, Mein R, Cullup T, Dionisi-Vici C, Al-Gazali L, Al-Owain M, Bruwer Z, Al Thihli K, El-Garhy R, Flanigan KM, Manickam K, Zmuda E, Banks W, Gershoni-Baruch R, Mandel H, Dagan E, Raas-Rothschild A, Barash H, Filloux F, Creel D, Harris M, Hamosh A, Kolker S, Ebrahimi-Fakhari D, Hoffmann GF, Manchester D, Boyer PJ, Manzur AY, Lourenco CM, Pilz DT, Kamath A, Prabhakar P, Rao VK, Rogers RC, Ryan MM, Brown NJ, McLean CA, Said E, Schara U, Stein A, Sewry C, Travan L, Wijburg FA, Zenker M, Mohammed S, Fanto M, Gautel M, Jungbluth H. 2016. EPG5-related Vici syndrome: a paradigm of neurodevelopmental disorders with defective autophagy. Brain 139:765-781.

Cullup T, Kho AL, Dionisi-Vici C, Brandmeier B, Smith F, Urry Z, Simpson MA, Yau S, Bertini E, McClelland V, Al-Owain M, Koelker S, Koerner C, Hoffmann GF, Wijburg FA, Hoedt AE, Rogers RC, Manchester D, Miyata R, Hayashi M, Said E, Soler D, Kroisel PM, Windpassinger C, Filloux FM, Al-Kaabi S, Hertecant J, Del Campo M, Buk S, Bodi I, Goebel HH, Sewry CA, Abbs S, Mohammed S, Josifova D, Gautel M, Jungbluth H. 2013. Recessive mutations in EPG5 cause Vici syndrome, a multisystem disorder with defective autophagy. Nat Genet 45:83-87.

Glass HC, Shaw GM, Ma C, Sherr EH. 2008. Agenesis of the corpus callosum in California 1983-2003: a population-based study. Am J Med Genet A 146A:2495-2500.

Glenn OA, Goldstein RB, Li KC, Young SJ, Norton ME, Busse RF, Goldberg JD, Barkovich AJ. 2005. Fetal magnetic resonance imaging in the evaluation of fetuses referred for sonographically suspected abnormalities of the corpus callosum. J Ultrasound Med 24:791-804.

Kane MS, Vilboux T, Wolfe LA, Lee PR, Wang Y, Huddleston KC, Vockley JG, Niederhuber JE, Solomon BD. 2016. Aberrant splicing induced by the most common EPG5 mutation in an individual with Vici syndrome. Brain 139:e52.

Marsh AP, Lukic V, Pope K, Bromhead C, Tankard R, Ryan MM, Yiu EM, Sim JC, Delatycki MB, Amor DJ, McGillivray G, Sherr EH, Bahlo M, Leventer RJ, Lockhart PJ. 2015. Complete callosal agenesis, pontocerebellar hypoplasia, and axonal neuropathy due to AMPD2 loss. Neurol Genet 1:e16.

Miyata R, Hayashi M, Itoh E. 2014. Pathological changes in cardiac muscle and cerebellar cortex in Vici syndrome. Am J Med Genet A 164A:3203-3205.

Rogers CR, Aufmuth B, Monesson S. 2011. Vici Syndrome: A Rare Autosomal Recessive Syndrome with Brain Anomalies, Cardiomyopathy, and Severe Intellectual Disability. Case Reports in Genetics Volume 2011.

Santo S, D'Antonio F, Homfray T, Rich P, Pilu G, Bhide A, Thilaganathan B, Papageorghiou AT. 2012. Counseling in fetal medicine: agenesis of the corpus callosum. Ultrasound Obstet Gynecol 40:513-521.

Tang PH, Bartha AI, Norton ME, Barkovich AJ, Sherr EH, Glenn OA. 2009. Agenesis of the corpus callosum: an MR imaging analysis of associated abnormalities in the fetus. AJNR 30:257-263.

Vici CD, Sabetta G, Gambarara M, Vigevano F, Bertini E, Boldrini R, Parisi SG, Quinti I, Aiuti F, Fiorilli M. 1988. Agenesis of the corpus callosum, combined immunodeficiency, bilateral cataract, and hypopigmentation in two brothers. Am J Med Genet A 29:1-8.

Zhao H, Zhao YG, Wang X, Xu L, Miao L, Feng D, Chen Q, Kovacs AL, Fan D, Zhang H. 2013. Mice deficient in Epg5 exhibit selective neuronal vulnerability to degeneration. JCB 200:731-741.

FIGURE AND TABLE LEGENDS

Figure 1 Fetal MRI and general macroscopic findings. A) T2-weighted image, axial plane on the level of the deep grey nuclei, showing absent callosal fibers crossing through the midline (asterisk), with abnormal widely open Sylvian fissures (arrow) and enlarged peri-cerebral spaces; **B)** T2-weighted image, mid-sagittal plane, demonstrating a small and insufficiently foliated vermis with enlargement of the cisterna magna (asterisk), and a flattened pons (white arrow); **C)** Right lateral view of the brain showing a triangular-shaped Sylvian fissure (black arrow) (instead of being half-closed at 30 weeks gestation), with no superior temporal gyrus (asterisk), a small cerebellum, flat pons and thin medulla. **D)** Coronal sections through the brain on the level of the temporal poles, showing reduction of the callosal fibers to a thin ribbon, with no apparent Probst bundles (black arrow).

Figure 2 Representative neurohistological findings. A) Histological section at the level of the genu of the corpus callosum, where only a few callosal fibres are identified (black arrow) (H&E stain, OM x 10); **B)** At higher magnification, callosal fibers are irregularly arranged, forming short and small Probst Bundles (H&E stain, OM x 100); **C)** Absent tertiary folia in the vermis, but with normal four-layered cerebellar cortex (H&E stain, OM x 10); **D)** In the mesencephalon, there is hypoplasia of the pes pedunculi, which are composed of several fascicles of irregular shape (black arrows) (H&E stain, OM x 25); **E)** In the medulla, pyramids are absent on the right, compared with an age-matched control (black arrow) (H&E stain, OM x 25); **F)** There is almost no myelination compared to the control, where myelination (blue colour) becomes diffuse at this age, in particular with regards to the median lemniscus (black arrow) (KB stain, OM x 100); **G)** Subcapsular anterior cataract of the left lens, characterized by proliferation of the anterior epithelium which is pluri-stratified (black arrow) instead of forming a single layer of cuboidal cells covered with an acellular band of connective tissue typically seen at a comparable gestational age (insert, thin arrow and thick

arrow respectively (HES stain, OM x 200, HE stain in the insert, OM x 200); **H)** There is no discoloration of the ciliary processes (black arrow) and of the retinal pigmentary epithelium (asterisk) (HES stain, OM x 200). H&E = haematoxylin and eosin stain); OM = original magnification; KB = Klüver-Barrera (cresyl violet-luxol fast blue) stain; HES = haematoxylin-eosin-saffron stain.

Supplemental Table ST1 Autopsy features in 5 cases with *EPG5*-related Vici syndrome.

WG = weeks of gestation; NS = not specified; CC = corpus callosum.

CONFLICT OF INTEREST

The authors do not have any conflict of interest to declare.

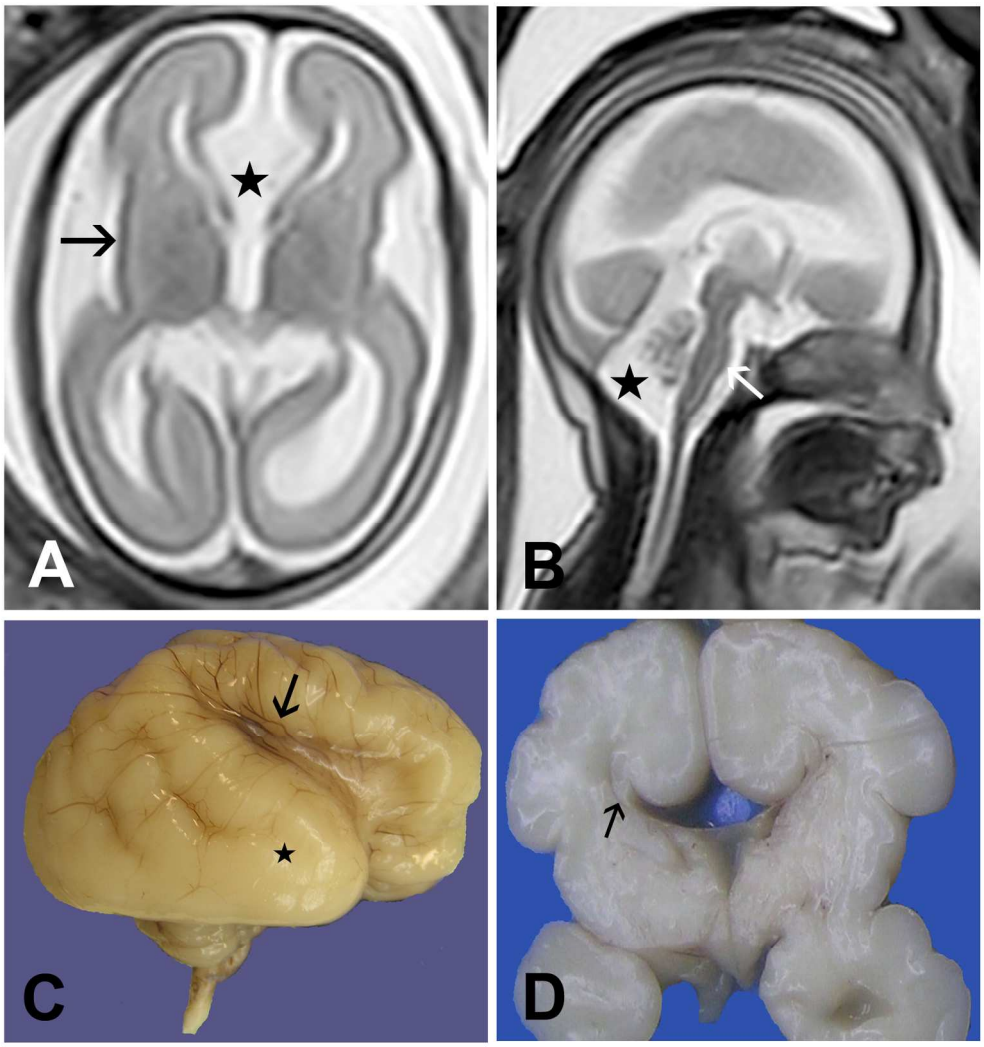

Figure 1
Fetal MRI and general macroscopic findings. A) T2-weighted image, axial plane on the level of the deep grey nuclei, showing absent callosal fibers crossing through the midline (asterisk), with abnormal widely open Sylvian fissures (arrow) and enlarged peri-cerebral spaces; B) T2-weighted image, mid-sagittal plane, demonstrating a small and insufficiently foliated vermis with enlargement of the cisterna magna (asterisk), and a flattened pons (white arrow); C) Right lateral view of the brain showing a triangular-shaped Sylvian fissure (black arrow) (instead of being half-closed at 30 weeks gestation), with no superior temporal gyrus (asterisk), a small cerebellum, flat pons and thin medulla. D) Coronal sections through the brain on the level of the temporal poles, showing reduction of the callosal fibers to a thin ribbon, with no apparent Probst bundles (black arrow).

165x176mm (300 x 300 DPI)

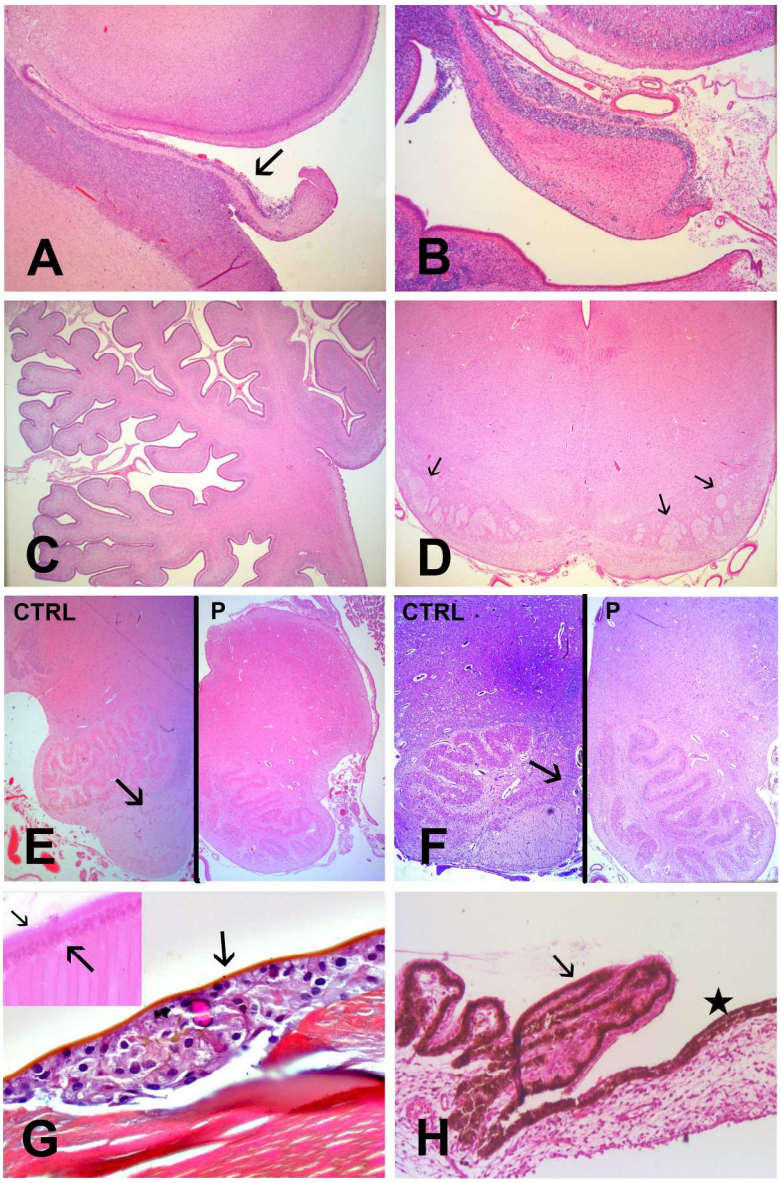

Figure 2 Representative neurohistological findings. A) Histological section at the level of the genu of the corpus callosum, where only a few callosal fibres are identified (black arrow) (H&E stain, OM x 10); B) At higher magnification, callosal fibers are irregularly arranged, forming short and small Probst Bundles (H&E stain, OM x 100); C) Absent tertiary folia in the vermis, but with normal four-layered cerebellar cortex (H&E stain, OM x 10); D) In the mesencephalon, there is hypoplasia of the pes pedunculi, which are composed of several fascicles of irregular shape (black arrows) (H&E stain, OM x 25); E) In the medulla, pyramids are absent on the right, compared with an age-matched control (black arrow) (H&E stain, OM x 25); F) There is almost no myelination compared to the control, where myelination (blue colour) becomes diffuse at this age, in particular with regards to the median lemniscus (black arrow) (KB stain, OM x 100); G) Subcapsular anterior cataract of the left lens, characterized by proliferation of the anterior epithelium which is pluri-stratified (black arrow) instead of forming a single layer of cuboidal cells covered with an acellular band of connective tissue typically seen at a comparable gestational age (insert, thin arrow and thick arrow respectively (HES stain, OM x 200, HE stain in the insert, OM x 200); H) There is no discoloration of the

ciliary processes (black arrow) and of the retinal pigmentary epithelium (asterisk) (HES stain, OM x 200). H&E = haematoxylin and eosin stain); OM = original magnification; KB = Klüver-Barrera (cresyl violet-luxol fast blue) stain; HES = haematoxylin-eosin-saffron stain.

169x251mm (300 x 300 DPI)

POST MORTEM EXAMINATION – METHODS

Fetal biometric data

Fetal biometric data were evaluated according to Guihard-Costa et al. [Guihard-Costa and others 2002]. Brain growth and maturation were evaluated according to the criteria of Guihard-Costa et al., and of Fees Higgins and colleagues [Feess-Higgins and Larroche 1988; Guihard-Costa and Larroche 1990]. Occipito-frontal circumference normal fetal reference values were from Garel et al. [Garel 2000]. Postnatal brain biometric data as summarized in Supplemental Table ST1 were evaluated according to Ludwig [Ludwig 2002].

Brain and muscle tissue preparation and analysis

The brain was fixed in a 10% formalin-zinc buffer solution for one month. Multiple 7 µm sections were processed from the cerebral hemispheres, mesencephalon, pons, medulla, cerebellar vermis and the dentate nuclei. Tissue sections were stained with Haematoxylin-Eosin (H&E), Klüver-Barrera and periodic acid Schiff (PAS). Immunohistochemistry was performed on telencephalic structures and cerebellum using MAP2 (Diluted 1/50, Sigma Aldrich) and phosphorylated Neurofilaments antibodies (diluted 1/200, Dakopatts). Quadriceps muscle was not available, but a psoas muscle sample had been obtained and kept frozen at -80°C. Ten µm cryostat sections were stained with haematoxylin-eosin and the modified Gomori method trichrome. Six µm sections from the muscle and cardiac frozen samples were immunolabelled by antibodies directed against β-spectrin (NCL-spec1, diluted 1/50, Menarini Novocastra, Le Perray en Yvelines, France), ubiquitin (diluted 1/200, Dakopatts, Trappes, France), p62 (diluted 1/1000, BD biosciences, le Pont de Claix, France), myosin S, F, D and N (diluted 1/80, 1/40, 1/40 and 1/60 respectively, Menarini Novocastra) and LC3 (diluted 1/200, Interchim, Montluçon, France). Incubations were performed for 32

minutes at room temperature using the Ventana Benchmark XT system. Slides were then processed by the Ultraview Universal DAB detection kit (Ventana). All immunohistochemical stains were compared with an age matched control case examined after a spontaneous abortion for premature rupture of the membranes whose muscle and heart were histologically normal. Transmission electron microscopy was also carried out on heart and psoas muscles according to standardized protocols.

References

Feess-Higgins A, Larroche J-C. 1988. Development of the human fetal brain: An anatomical atlas. Paris: Masson.

Garel C. 2000. Le développement du cerveau foetal : Atlas IRM et biométrie. Sauramps Médical p152.

Guihard-Costa AM, Larroche JC. 1990. Differential growth between the fetal brain and its infratentorial part. Early Hum Dev 23(1):27-40.

Guihard-Costa AM, Menez F, Delezoide AL. 2002. Organ weights in human fetuses after formalin fixation: standards by gestational age and body weight. Pediatr Dev Pathol 5(6):559-578.

Ludwig J. 2002. Handbook of autopsy practice. . Berlin: Springer.

Cases	Brain Weight	Brain macroscopy	Brain histological findings	Associated lesions
Dionisi Vici et al., 1988 3 years	596g Extreme microcephaly	Ventricular dilatation CC agenesis Cerebellar vermis hypoplasia	CC agenesis with Probst bundles No other lesions	Thymus and lymphoid tissue hypoplasia Cardiac left ventricular dilatation Endocardial fibroelastosis
Rogers et al., 2011 8 years	NS Microcephaly	CC agenesis Cerebellar vermis hypoplasia	Focal loss of Purkinje and internal grain layer cells Occipital polymicrogyria Retinal hypopigmentation	Absent thyroid Hypoplastic thymus Cardiac biventricular dilatation
Miyata et al., 2014 8 months	605g Microcephaly	CC agenesis Pontocerebellar hypoplasia	CC agenesis Pyramidal tract hypoplasia Purkinje cell torpedoes Axonal swellings in the internal granular layer Reduced transverse pontine fibres	Vacuolated cardiomyocytes Cutaneous albinism
Byrne et al., 2016 11 months	550g Extreme microcephaly	CC agenesis Opened Sylvian fissures Abnormal gyri with profound sulci	CC agenesis with Probst bundles Hypoplastic hippocampi Reduced white matter Pyramidal tract hypoplasia PAS storage material in Purkinje cells	NS
Present case 30 WG	179g, (<3rd percentile) Microcephaly	Opened Sylvian fissures Delayed gyration CC agenesis Ponto-cerebellar hypoplasia	Extreme CC hypoplasia Probst bundles Delayed foliation of the vermis Pyramidal tract hypoplasia Normal pigmentation of the retina	Cataract Hypoplastic external male genitalia Cardiac hypertrophy/dilatation Pale cardiomyocytes

Supplemental Table 1 ST1

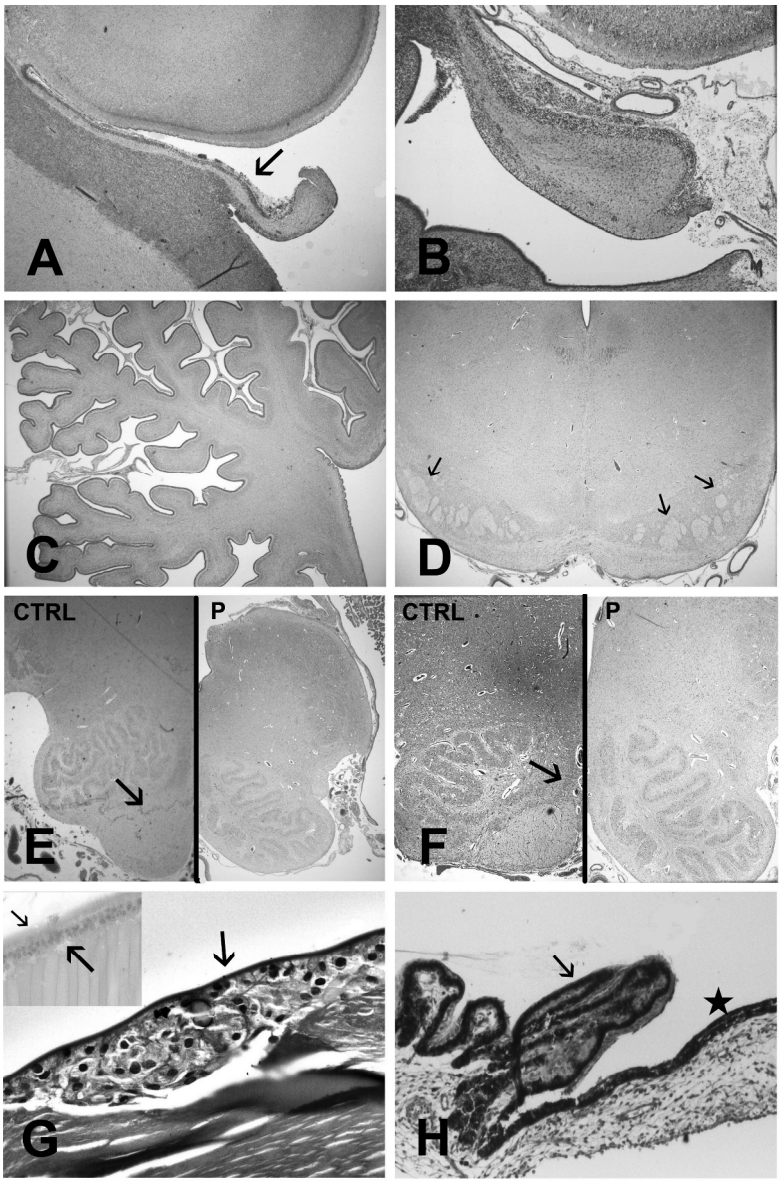

Figure 2 Representative neurohistological findings. A) Histological section at the level of the genu of the corpus callosum, where only a few callosal fibres are identified (black arrow) (H&E stain, OM x 10); B) At higher magnification, callosal fibers are irregularly arranged, forming short and small Probst Bundles (H&E stain, OM x 100); C) Absent tertiary folia in the vermis, but with normal four-layered cerebellar cortex (H&E stain, OM x 10); D) In the mesencephalon, there is hypoplasia of the pes pedunculi, which are composed of several fascicles of irregular shape (black arrows) (H&E stain, OM x 25); E) In the medulla, pyramids are absent on the right, compared with an age-matched control (black arrow) (H&E stain, OM x 25); F) There is almost no myelination compared to the control, where myelination (blue colour) becomes diffuse at this age, in particular with regards to the median lemniscus (black arrow) (KB stain, OM x 100); G) Subcapsular anterior cataract of the left lens, characterized by proliferation of the anterior epithelium which is pluri-stratified (black arrow) instead of forming a single layer of cuboidal cells covered with an acellular band of connective tissue typically seen at a comparable gestational age (insert, thin arrow and thick arrow respectively (HES stain, OM x 200, HE stain in the insert, OM x 200); H) There is no discoloration of the

ciliary processes (black arrow) and of the retinal pigmentary epithelium (asterisk) (HES stain, OM x 200). H&E = haematoxylin and eosin stain); OM = original magnification; KB = Klüver-Barrera (cresyl violet-luxol fast blue) stain; HES = haematoxylin-eosin-saffron stain.

169x251mm (300 x 300 DPI)